Journal of Process Control 20 (2010) 922–933

Contents lists available at ScienceDirect

Journal of Process Control

journal homepage: www.elsevier.com/locate/jprocont

Independent design of multi-loop PI/PID controllers for interacting multivariable processes

Truong Nguyen Luan Vu, Moonyong Lee*

School of Chemical Engineering and Technology, Yeungnam University, Daedong 214-1, Kyongsan, Kyongbuk 712-749, South Korea

ARTICLE INFO

Article history:
Received 2 January 2010
Received in revised form 26 April 2010
Accepted 14 June 2010

Keywords:
Multi-loop PI/PID controller tuning
Effective open-loop transfer function (EOTF)
Model reduction
Internal model control (IMC)
Dynamic relative gain array

ABSTRACT

The interactions between input/output variables are a common phenomenon and the main obstacle encountered in the design of multi-loop controllers for interacting multivariable processes. In this study, a novel method for the independent design of multi-loop PI/PID controllers is proposed. The idea of an effective open-loop transfer function (EOTF) is first introduced to decompose a multi-loop control system into a set of equivalent independent single loops. Using a model reduction technique, the EOTF is further approximated to the reduced-order form. Based on the corresponding EOTF model, the individual controller of each single loop is then independently designed by applying the internal model control (IMC)-based PID tuning approach for single-input/single-output (SISO) systems, while the main effects of the dynamic interactions are properly taken into account. Several illustrative examples are employed to demonstrate the effectiveness of the proposed method.

1. Introduction

Most chemical processes are basically multi-input/multi-output (MIMO) systems. Despite the development of advanced multivariable controllers, the multi-loop PI/PID control using multiple single-input/single-output (SISO) PI/PID controllers remains the standard for controlling MIMO systems with modest interaction because of its simple and failure tolerant structure and adequate performance [1,2]. However, due to process and loop interactions, the design and tuning of multi-loop controllers is much more difficult compared with that of single-loop controllers. Since the controllers interact with each other, the tuning of one loop cannot be done independently. Applying the tuning methods for a SISO system to multi-loop systems often leads to poor performance and stability. Much research has been focused on how to efficiently take loop interactions into account in the multi-loop controller design. Many methods have been proposed, including the detuning method, sequential loop closing (SLC) method, relay auto-tuning method, and independent loop method.

The biggest log modulus tuning (BLT) method proposed by Luyben [3] is a typical example of the detuning method, wherein each individual controller is first designed based on the Ziegler–Nichols (Z–N) tuning rules [4] by ignoring process interactions from other loops. Then, the interactions are taken into account by detuning each controller until the multivariable Nyquist stability is satisfied. The attractiveness of this method is due to the simplicity in implementation and comprehensibleness for control engineers. However, a disadvantage is that the controller settings are made more conservative.

The well-known SLC method for the design of multi-loop controllers was first introduced by Mayne [5] and later studied by Hovd and Skogestad [6]. In this method, the controllers are tuned sequentially, wherein the controller of the fastest loops should be tuned first by considering a selected input–output pair; this loop is then closed and then the controller of the lower loops is tuned for a second pair while the first control loop remains closed and so on. The SLC method is simpler than the detuning method as each controller is designed using SISO design methods.

In relay auto-tuning for the multi-loop control system [7–10], the relay feedback technique is applied to the design of each corresponding SISO controller. The control loops are tuned sequentially or simultaneously. Furthermore, on the basis of sequential algorithm, the multi-loop control system is designed in a sequence of SISO design problems and the interaction taken into account in a sequential fashion. In this way, Loh et al. [8] and Shen and Yu [9] have directly combined the efficiency of a single-loop relay and SLC method to design multi-loop controllers, which is sometimes called as the auto-tuning SLC method. These methods require minimal process information but tuning sequence has to be repeated for the correct sequence if the design sequence is not appropriate.

The independent loop method is used to surmount the restriction of the relay auto-tuning. As discussed by a number of authors

* Corresponding author. Tel.: +82 53 810 2512; fax: +82 53 811 3262.
E-mail address: mynlee@yu.ac.kr (M. Lee).

0959-1524/$ – see front matter © 2010 Elsevier Ltd. All rights reserved.
doi:10.1016/j.jprocont.2010.06.012

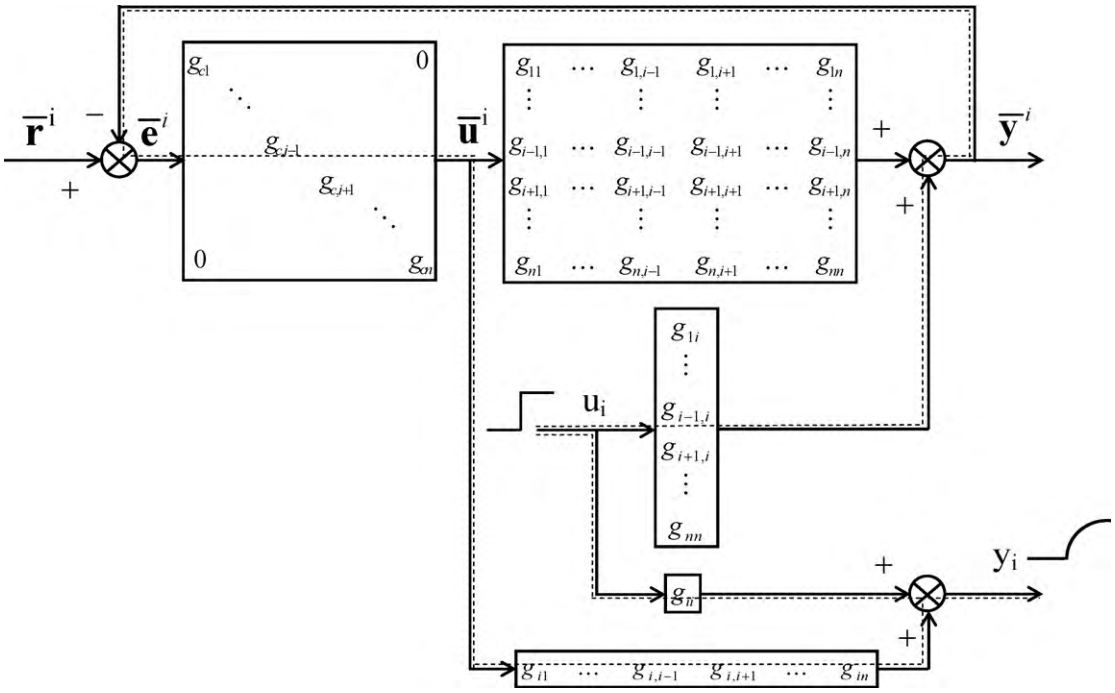

Fig. 1. Block diagram for the concept of the effective open-loop transfer function in a $n \times n$ multi-loop system: loop i is open while all other loops are closed.

[11–14], the independent loop method has a potential advantage in that the failure tolerance of the overall control system is automatically guaranteed, wherein each controller is independently designed based on the corresponding open-loop and closed-loop transfer functions, thereby satisfying the inequality constraints on the process interactions [11]. A potential disadvantage of the method is one of the conservatism due to the inherent assumption of the independent design, which does not exploit the information regarding controllers in other loops [12]. For this, the independent loop method for IMC type multi-loop controllers [13,14] is used to reduce the conservatism.

Recently, several researchers have introduced the concept of an effective open-loop transfer function (EOTF) to take into account the loop interactions in the novel design of a multi-loop controller [15–19]. Using this concept, the design of a multi-loop controller can be reasonably converted to the design of a single-loop controller. On the basis of structure decomposition, the multi-loop control system is completely separated into equivalent individual SISO loops, and thus the effects of the process and controller on the loop interaction and subsequent system properties, such as right half plane (RHP) zeros and poles, integrity, and stability, are elucidated [15]. Moreover, He et al. [16] have suggested the dynamic relative interaction to derive the multiplicative model factor (MMF) for an individual control loop; the equivalent transfer function is then obtained by multiplying the original loop transfer function with the approximated MMF within the neighborhood of the individual control loop critical frequency. Huang et al. [17] found that the EOTF is formulated without prior knowledge of controller dynamics in other loops and that the controller is independently designed for equivalent single loops. In an alternate manner, Xiong and Cai [18] suggested that the EOTF provides both gain and phase information for multi-loop controller design in four ways. The advantages of the EOTF involve reduced modeling requirements and ease of implementation while the potential disadvantage is reduction in achievable control performance due to restricted controller structure [19].

The control performance of the multi-loop systems is also closely related to the control loop pairing. Given its clear and useful definition, the well-known RGA [20] has been widely used for the multi-loop structure design, such as a ratio of an open-loop

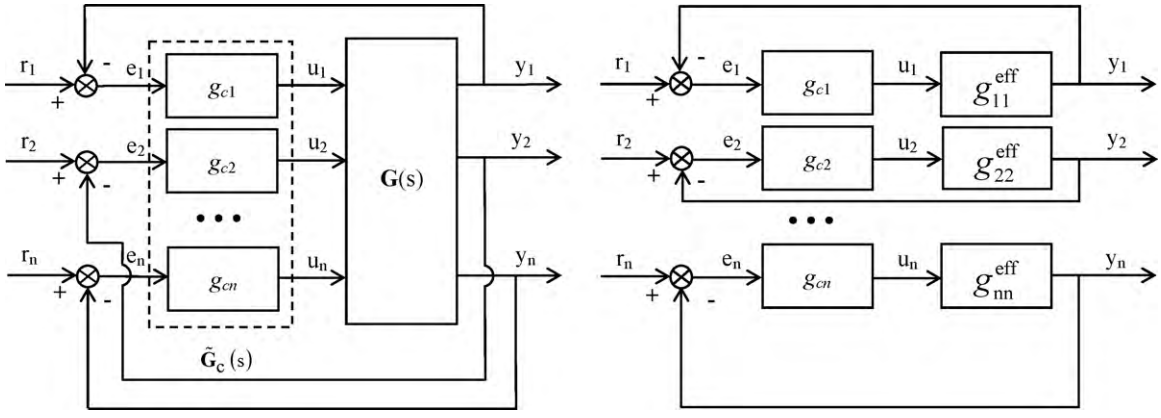

Fig. 2. Multi-loop system and equivalent independent SISO systems with the corresponding EOTFs.

gain to a closed-loop gain. The definition of RGA was extended to dynamic RGA (DRGA), with frequency-dependent terms, by replacing the steady-state gains with the corresponding transfer functions [21–24]. Xiong et al. [25] proposed the relative effective gain array (REGA) by employing the steady-state gain and bandwidth of the process transfer function element that combines the benefits of both the RGA and DRGA. He et al. [26] suggested the relative normalized gain array (RNGA) for loop interaction measurements. Since this takes into account both the steady-state and transient information of the process transfer function, it provides more accurate interaction assessment than the conventional RGA-based loop paring criterion.

In this paper, an efficient approach to incorporate the loop interaction effect into the design of multi-loop PI/PID controllers is proposed by utilizing the concept of the EOTF. Based on the characteristics of the closed-loop dynamics, the effect of other loops upon the particular loop is effectively expressed in terms of the DRGA with no need of *a priori* information of other controllers. A multi-loop control system is then decomposed into a set of independent SISO loops represented by corresponding EOTFs; the tuning of the multi-loop PI/PID controller is thus converted to the design of independent single-loop PI/PID controllers. Several illustrated simulation examples are employed to demonstrate the effectiveness of the proposed method for various interacting multivariable processes.

2. Effective open-loop transfer function and dynamic relative gain

Consider the open-loop stable multi-loop system in Fig. 1, where $\bar{\mathbf{r}}^i$, $\bar{\mathbf{u}}^i$, and $\bar{\mathbf{y}}^i$ are the set-point, manipulated, and controlled variable vectors, where r_i, u_i, and y_i are discarded from $\mathbf{r}$, $\mathbf{u}$, and $\mathbf{y}$, respectively. Let the EOTF of loop i be defined as the transfer function relating u_i with y_i where loop i is open while all other loops are closed. Fig. 1 shows the block diagram for the concept of the EOTF of loop i. The EOTF differs from the original open-loop transfer function (OTF) by transmission interaction through a path including other loops. It is clear that the EOTF corresponds to the actual open-loop transfer function under multi-loop situations and thus, tuning of the controller of loop i should be done based on the EOTF, g_{ii}^{eff}, rather than the original OTF, g_{ii}. Furthermore, as shown in Fig. 2, a multi-loop MIMO system can be considered a set of n independent SISO systems with corresponding EOTFs.

From the block diagram in Fig. 1 with $\bar{\mathbf{r}}^i = 0$, $\bar{\mathbf{u}}^i$ is obtained by

$$\bar{\mathbf{u}}^i = -\tilde{\mathbf{G}}_c^i \bar{\mathbf{y}}^i = -\tilde{\mathbf{G}}_c^i (\bar{\mathbf{g}}^{ic} u_i + \bar{\mathbf{G}}^i \bar{\mathbf{u}}^i) \tag{1}$$

where $\tilde{\mathbf{G}}_c^i$ denotes a multi-loop controller matrix in which g_{ci} is dropped from $\tilde{\mathbf{G}}_c$. $\bar{\mathbf{G}}^i$ denotes a transfer function matrix where both the ith row and column are removed from $\mathbf{G}$. The terms $\bar{\mathbf{g}}^{ir}$ and $\bar{\mathbf{g}}^{ic}$ denote the ith row and column vector of matrix $\mathbf{G}$ where g_{ii} is discarded, respectively.

Rearranging (1) yields

$$\bar{\mathbf{u}}^i = -\tilde{\mathbf{G}}_c^i (\mathbf{I} + \bar{\mathbf{G}}^i \tilde{\mathbf{G}}_c^i)^{-1} \bar{\mathbf{g}}^{ic} u_i \tag{2}$$

Therefore, the relation between y_i and u_i is written as

$$y_i = g_{ii} u_i + \bar{\mathbf{g}}^{ir} \bar{\mathbf{u}}^i = [g_{ii} - \bar{\mathbf{g}}^{ir} \tilde{\mathbf{G}}_c^i (\mathbf{I} + \bar{\mathbf{G}}^i \tilde{\mathbf{G}}_c^i)^{-1} \bar{\mathbf{g}}^{ic}] u_i \tag{3}$$

The complication of the dynamic interaction is clear from (3). The open-loop dynamics between y_i and u_i depend not only upon the single transfer function, g_{ii}, but also on the process and controller terms in all other loops. This also implies that in principle, tuning of one controller cannot be done independently and depends on other controllers. However, this complicated relation due to the dynamic interaction can be reasonably simplified by introducing several assumptions. Assuming that the controllers include integral actions to avoid offset and that the closed-loop dynamics, by properly tuned controllers, are sufficiently faster than the open-loop dynamics, then a perfect control approximation, $\bar{\mathbf{G}}^i \tilde{\mathbf{G}}_c^i (\mathbf{I} + \bar{\mathbf{G}}^i \tilde{\mathbf{G}}_c^i)^{-1} = \mathbf{I}$, can be considered at frequencies lower than the cross-over frequency. Therefore, (3) is reasonably simplified as follows

$$\begin{aligned} y_i &= [g_{ii} - \bar{\mathbf{g}}^{ir} (\bar{\mathbf{G}}^i)^{-1} \bar{\mathbf{G}}^i \tilde{\mathbf{G}}_c^i (\mathbf{I} + \bar{\mathbf{G}}^i \tilde{\mathbf{G}}_c^i)^{-1} \bar{\mathbf{g}}^{ic}] u_i \\ &= [g_{ii} - \bar{\mathbf{g}}^{ir} (\bar{\mathbf{G}}^i)^{-1} \bar{\mathbf{g}}^{ic}] u_i = g_{ii}^{\text{eff}} u_i \end{aligned} \tag{4}$$

Note that the EOTF of loop i, g_{ii}^{eff}, consists of a process dynamics term only and does not include knowledge of other controllers.

Furthermore, the EOTF can be compactly expressed in terms of the DRGA, as follows (see details of derivation in Appendix A)

$$g_{ii}^{\text{eff}} = \frac{g_{ii}}{\Lambda_{ii}} \tag{5}$$

where Λ_{ii} denotes the ith diagonal element of the DRGA and is calculated by

$$\Lambda_{ii} = [\mathbf{G} \otimes (\mathbf{G}^{-1})^T]_{ii} \tag{6}$$

where the symbol $\otimes$ denotes the element by element multiplication (Hadamard or Schur product) and the superscript T designates the transpose of a matrix.

The physical meaning of DRGA is clearly indicated from (5): the ith diagonal element of the DRGA implies a ratio of the open-loop transfer function to the effective open-loop transfer functions of loop i, under the assumption of perfect control of other loops.

In this paper, the derivation of the EOTF and its physical meaning have been discussed in a different transparent way from the previous works [15–19].

3. Reduced EOTF for controller design

One of the most common approaches for controller design is to use a reduced-order model that simplifies the process dynamics. Since the EOTF is likely to show a complicated dynamic model form, the approach using a reduced-order model is generally required. Any conventional model reduction technique can be applied for this purpose. In this section, a simple model reduction technique is applied to approximate the EOTF to a reduced-order model, such as the first-order plus dead time (FOPDT) and the second-order plus dead time (SOPDT) models.

A two-input, two-output (TITO) multi-delay process is one of the most commonly encountered multivariable processes in the process industry [27–29]. A large number of previous studies focused on designing multi-loop control system of TITO processes. For a 2×2 system, the general stable square transfer function matrix is represented as

$$\mathbf{G}(s) = \begin{bmatrix} g_{11}(s) & g_{12}(s) \\ g_{21}(s) & g_{22}(s) \end{bmatrix} \tag{7}$$

The DRGA obtained from (6) is

$$\Lambda_{11}(s) = \Lambda_{22}(s) = \left(\frac{g_{11}(s) g_{22}(s)}{g_{11}(s) g_{22}(s) - g_{12}(s) g_{21}(s)} \right) \tag{8}$$

Therefore, the EOTFs for the first and second loops are found using (5), respectively:

$$g_{11}^{\text{eff}}(s) = g_{11}(s) - \frac{g_{12}(s) g_{21}(s)}{g_{22}(s)} \tag{9}$$

$$g_{22}^{\text{eff}}(s) = g_{22}(s) - \frac{g_{12}(s) g_{21}(s)}{g_{11}(s)} \tag{10}$$

For a 3×3 system, the derivation of EOTF is substantiated in a similar manner as that of the 2×2 system. The diagonal elements of the DRGA are established from (6) as follows

$$\Lambda_{11} = \frac{g_{11}(g_{22}g_{33} - g_{23}g_{32})}{g_{11}g_{22}g_{33} + g_{21}g_{13}g_{32} + g_{31}g_{12}g_{23} - g_{11}g_{23}g_{32} - g_{21}g_{12}g_{33} - g_{31}g_{13}g_{22}} \quad (11)$$

$$\Lambda_{22} = \frac{g_{22}(g_{11}g_{33} - g_{13}g_{31})}{g_{11}g_{22}g_{33} + g_{21}g_{13}g_{32} + g_{31}g_{12}g_{23} - g_{11}g_{23}g_{32} - g_{21}g_{12}g_{33} - g_{31}g_{13}g_{22}} \quad (12)$$

$$\Lambda_{33} = \frac{g_{33}(g_{11}g_{22} - g_{12}g_{21})}{g_{11}g_{22}g_{33} + g_{21}g_{13}g_{32} + g_{31}g_{12}g_{23} - g_{11}g_{23}g_{32} - g_{21}g_{12}g_{33} - g_{31}g_{13}g_{22}} \quad (13)$$

Thus, the EOTFs for the first, second, and third loops are constituted as

$$g_{11}^{\text{eff}} = g_{11} - \left[\frac{(g_{12}g_{21}g_{33} + g_{12}g_{23}g_{31}) - (g_{13}g_{31}g_{22} + g_{13}g_{32}g_{21})}{g_{22}g_{33} - g_{23}g_{32}}\right] \quad (14)$$

$$g_{22}^{\text{eff}} = g_{22} - \left[\frac{(g_{12}g_{21}g_{33} + g_{13}g_{32}g_{21}) - (g_{23}g_{32}g_{11} + g_{23}g_{31}g_{12})}{g_{11}g_{33} - g_{13}g_{31}}\right] \quad (15)$$

$$g_{33}^{\text{eff}} = g_{33} - \left[\frac{(g_{13}g_{31}g_{22} + g_{12}g_{23}g_{31}) - (g_{23}g_{32}g_{11} + g_{13}g_{32}g_{21})}{g_{11}g_{22} - g_{12}g_{21}}\right] \quad (16)$$

As seen from the equations above, the resulting EOTFs are usually too complicate to be directly utilized for the controller design. To overcome this difficulty, the EOTFs have to be simplified to low-order models, such as FOPDT and SOPDT. A lot of model reduction techniques are available, including, but not limited to, the least squares algorithm [30–32], polynomial approximation [33], Laguerre expansion [34–36], and the Gaussian frequency domain approach [37]. Any technique can be applied toward fitting the EOTFs into a low-order model.

In this work, for the purpose of evaluating the proposed EOTF, a simple model reduction technique was proposed based on the coefficient matching method.

Expanding g_{ii}^{eff} in a Maclaurin series in s gives

$$g_{ii}^{\text{eff}}(s) = a_{ii} + b_{ii}s + c_{ii}s^2 + d_{ii}s^3 + e_{ii}s^4 + O(s^5) \quad (17)$$

where the coefficients of this polynomial are

$$a_{ii} = g_{ii}^{\text{eff}}(0) \quad (18a)$$

$$b_{ii} = \left.\frac{dg_{ii}^{\text{eff}}(s)}{ds}\right|_{s=0} \quad (18b)$$

$$c_{ii} = \frac{1}{2}\left.\frac{d^2g_{ii}^{\text{eff}}(s)}{ds^2}\right|_{s=0} \quad (18c)$$

$$d_{ii} = \frac{1}{6}\left.\frac{d^3g_{ii}^{\text{eff}}(s)}{ds^3}\right|_{s=0} \quad (18d)$$

$$e_{ii} = \frac{1}{24}\left.\frac{d^4g_{ii}^{\text{eff}}(s)}{ds^4}\right|_{s=0} \quad (18e)$$

Since the FOPDT model is most widely used for modeling monotonic stable dynamics, given its simplicity with reasonable performance, the FOPDT dynamics as a reduced-order model must be considered first.

$$g^{r\_\text{eff}} = \frac{Ke^{-\theta s}}{\tau s + 1} \quad (19)$$

Expanding the reduced EOTF given by (19) in a Maclaurin series in s also gives

$$g^{r\_\text{eff}}(s) = K - K(\theta + \tau)s + K\left[\frac{1}{2}\theta^2 + (\theta + \tau)\tau\right]s^2 + O(s^3) \quad (20)$$

Table 1
Relations between process parameters and polynomial coefficients for typical process models.

Model	Relations
$\frac{Ke^{-\theta s}}{\tau s+1}$	$K = a_{ii}$; $(\theta+\tau) = \left(-\frac{b_{ii}}{a_{ii}}\right)$; $\left[\frac{\theta^2}{2} + (\theta+\tau)\tau\right] = \left(\frac{c_{ii}}{a_{ii}}\right)$
$\frac{(\pm\tau_a s+1)Ke^{-\theta s}}{(\tau_1 s+1)(\tau_2 s+1)}$	$K = a_{ii}$; $(X_0 \mp \tau_a) = \left(-\frac{b_{ii}}{a_{ii}}\right)$; $[X_1 + X_0(\tau_2 \mp \tau_a)] = \left(\frac{c_{ii}}{a_{ii}}\right)$; $[X_2 + X_3(\tau_2 \mp \tau_a)] = \left(-\frac{d_{ii}}{a_{ii}}\right)$; $[X_4 + X_5(\tau_2 \mp \tau_a)] = \left(\frac{e_{ii}}{a_{ii}}\right)$

where $X_0 = \theta + \tau_1 + \tau_2$, $X_1 = (\theta^2/2) + (\theta + \tau_1)\tau_1$, $X_2 = (\theta^3/6) + ((\theta^2/2) + (\theta + \tau_1)\tau_1)\tau_1$, $X_3 = (\theta^2/2) + (\theta + \tau_1)\tau_1 + (\theta + \tau_2)\tau_2 + \tau_1\tau_2$, $X_4 = (\theta^4/24) + (((\theta^3/6) + (\tau_1\theta^2/2) + \tau_1{}^2\theta + \tau_1{}^3)\tau_1$, $X_5 = (\theta^3/6) + (\tau_1\theta^2/2) + \tau_1{}^2\theta + \tau_1{}^3 + (\tau_2\theta^2/2) + \tau_2{}^2\theta + \tau_2{}^3 + \tau_2\tau_1\theta + \tau_2\tau_1{}^2 + \tau_2{}^2\tau_1$.

where K, τ, and θ should be identified to approximate g_{ii}^{eff} as close as possible over control relevant frequency ranges. Comparing the first, second, and third terms of (20) with those of (17) leads to the following explicit equations for K, τ, and θ:

$$K = a_{ii} \quad (21a)$$

$$\tau = \sqrt{\frac{2c_{ii}}{a_{ii}} - \left(\frac{b_{ii}}{a_{ii}}\right)^2} \quad (21b)$$

$$\theta = -\frac{b_{ii}}{a_{ii}} - \sqrt{\frac{2c_{ii}}{a_{ii}} - \left(\frac{b_{ii}}{a_{ii}}\right)^2} \quad (21c)$$

In order for the resulting FOPDT model to be feasible, τ and θ should be real and positive. It is clear from (21) that the following condition should be satisfied for feasible τ and θ values:

$$\sqrt{\frac{2c_{ii}}{a_{ii}}} > \left(-\frac{b_{ii}}{a_{ii}}\right) > \sqrt{\frac{2c_{ii}}{a_{ii}} - \left(\frac{b_{ii}}{a_{ii}}\right)^2} \quad (22)$$

When the EOTF dynamics is too complicated to be properly expressed by a simple FOPDT model, reduction to the FOPDT model results in infeasible τ and/or θ values that are negative or complex. As such, the FOPDT model is not valid for approximating the EOTF dynamics and as such, more general dynamics such as a SOPDT model has to be considered. It has been shown from previous works [17,38–40] that a SOPDT model with a negative/positive zero satisfactorily represents most of the complicated process dynamics for the control relevant purpose.

$$g^{r\_\text{eff}} = \frac{(\pm\tau_a s + 1)Ke^{-\theta s}}{(\tau_1 s + 1)(\tau_2 s + 1)} \quad (23)$$

The relations between the polynomial coefficients and the process parameters for the SOPDT model are listed in Table 1. The SOPDT model parameter values of τ_1, τ_2, τ_a, and θ can also be obtained from those relations.

It is important to predict when τ and/or θ of the FOPDT model becomes infeasible in the proposed model reduction method. Suppose that the FOPDT model is attempted while the actual EOTF has the SOPDT dynamics given by (23). Accordingly, mathematical manipulation from the relations for the SOPDT process in Table 1 and the inequality constraint given by (22) provides the following conditions for when reduction to the FOPDT model leads to the infeasible parameter values:

For the case of SOPDT with a negative zero,

$$\tau_a > \sqrt{\tau_1^2 + \tau_2^2} \quad \text{or} \quad \frac{1}{2}\left[X_0 + \sqrt{2(\tau_1^2 + \tau_2^2) - X_0^2}\right] > \tau_a > \frac{1}{2}\left[X_0 - \sqrt{2(\tau_1^2 + \tau_2^2) - X_0^2}\right] \quad (24a)$$

For the case of SOPDT with a positive zero,

$$\tau_a > \sqrt{\tau_1^2 + \tau_2^2} \tag{24b}$$

where $X_0 = \theta + \tau_1 + \tau_2$.

For example, in the proposed model reduction method, either a large overshoot or a strong inverse response such as: $\tau_a > \sqrt{\tau_1^2 + \tau_2^2}$ causes infeasible τ and/or θ values in the FOPDT model. If the EOTF is monotonic and has no lead term, the proposed method always gives feasible τ and θ values. It should be noted that feasible parameter values do not guarantee accuracy of model reduction. Identification performance by any reduced-order model requires final confirmation by comparing the EOTF with the reduced EOTF.

4. Multi-loop PID controller design

Once a reduced EOTF is obtained, any PID tuning method for a SISO system can be applied for the design of each individual PID controller. In this study, the IMC-PID tuning rules suggested by Lee et al. [41] were chosen. The IMC-PID design approach is commonly used for the PID controller tuning in the process industry because of its many advantages, including simplicity, robust performance, and analytical form.

The overall procedure for driving the tuning rules of loop i is as follows:

First, the reduced EOTF, $g_{ii}^{r\text{-eff}}$, is decomposed to $g_{ii}^{r\text{-eff}} = p_{Ai}p_{Mi}$, where p_{Ai} and p_{Mi} are the non-minimum portion with an all-pass form and the minimum phase portion, respectively. The conventional IMC filter, f, is selected as: $f_i(s) = 1/(\lambda_i s + 1)^{m_i}$, in which λ_i is a design parameter that provides the tradeoff between performance and robustness. It is the desired closed-loop time constant for the set-point tracking. The filter order m_i is selected as a positive integer so that the controller is proper and realizable.

Then, the ideal feedback controller to yield the desired closed-loop response perfectly is given by

$$g_{ci} = \frac{q_i}{(1 - g_{ii}^{r\text{-eff}} q_i)} = \frac{p_{Mi}^{-1}(s)}{(\lambda_i s + 1)^{m_i} - p_{Ai}(s)} \tag{25}$$

where q_i is the IMC controller and is designed by: $q_i = p_{Mi}^{-1} f_i$.

Since the above resulting controller does not have a standard PID controller form, it is required to approximate the ideal feedback controller $\mathbf{G}_{ci}$ to the equivalent PID controller forms.

Expanding g_{ci} in a Maclaurin series in s yields

$$g_{ci} \equiv \frac{f_i(s)}{s} = \frac{1}{s}\left[f_i(0) + f_i'(0)s + \frac{f_i''(0)}{2!}s^2 + \frac{f_i'''(0)}{3!}s^3 + \cdots\right] \tag{26}$$

The controller given by (25) is interpreted as the standard PID controller by using the first three terms and truncating the higher order terms, given by

$$g_{ci}(s) = K_{ci}\left(1 + \frac{1}{\tau_{Ii}s} + \tau_{Di}s\right) \tag{27}$$

where

$$K_{ci} = f_i'(0) \tag{28a}$$

$$\tau_{Ii} = \frac{f_i'(0)}{f_i(0)} \tag{29b}$$

$$\tau_{Di} = \frac{f_i''(0)}{2f_i'(0)} \tag{28c}$$

The derivative and integral time constants computed from (27) could have negative values when the reduced EOTF model has a strong lead term. In this case, a PID controller in series with the first-order lag filter structure is recommended for use

$$g_{ci}(s) = K_{ci}\left(1 + \frac{1}{\tau_{Ii}s} + \tau_{Di}s\right)\frac{1}{\tau_{Fi}s + 1} \tag{29}$$

where

$$K_{ci} = -f_i(0)\left[\frac{f_i'''(0)}{3f_i''(0)}\right] + f_i'(0) \tag{30a}$$

$$\tau_{Ii} = -\frac{f_i'''(0)}{3f_i''(0)} + \frac{f_i'(0)}{f_i(0)} \tag{30b}$$

$$\tau_{Di} = \frac{1}{2}\left[\frac{2f_i'''(0)f_i'(0) - 3(f_i''(0))^2}{f_i'''(0)f_i(0) - 3f_i''(0)f_i'(0)}\right] \tag{30c}$$

$$\tau_{Fi} = -\frac{1}{3}\left[\frac{f_i'''(0)}{f_i''(0)}\right] \tag{30d}$$

5. Simulation study

In this section, three examples are considered to demonstrate the performance of the proposed method in comparison with those of other well-known methods. To ensure a fair comparison, the performance and robustness of the control system are measured by the following evaluation criteria.

5.1. Performance index

To evaluate closed-loop performance, the integral absolute error (IAE) criterion is considered, which is defined as:

$$\text{IAE} = \int_0^\infty |e(t)|dt \tag{31}$$

where $e(t) = r(t) - y(t)$.

5.2. Robustness index

In this study, a well-known method for robust stability [2,24,42,43] is utilized for a fair comparison with other comparative methods. The multiple sources of uncertainty are lumped into a single complex perturbation (multiplicative input/output form). Since the output uncertainty is often less restrictive than input uncertainty in terms of control performance [24], the robust stability of multi-loop control systems is examined under output multiplication uncertainty. For a process with an output uncertainty of $[\mathbf{I} + \Delta_0(s)]\mathbf{G}(s)$, the upper bound of the robust stability is given as [43]:

$$\gamma = \bar{\sigma}(\Delta_0) < 1/\bar{\sigma}[(\mathbf{I} + \mathbf{G}(j\omega)\tilde{\mathbf{G}}_c(j\omega))^{-1}\mathbf{G}(j\omega)\tilde{\mathbf{G}}_c(j\omega)] < \underline{\sigma}[\mathbf{I} + (\mathbf{G}(j\omega)\tilde{\mathbf{G}}_c(j\omega))^{-1}], \quad \forall\omega \geq 0 \tag{32}$$

where γ represents the degree of robust stability, Δ_0 perturbation as a multiplicative output, and $\bar{\sigma}$ and $\underline{\sigma}$ maximum and minimum singular values, respectively. It should be noted that: $\mathbf{G}(j\omega)\tilde{\mathbf{G}}_c(j\omega)$ is invertible.

For a fair comparison, all of the controllers being compared were designed to have the same degree of robust stability in terms of the γ value throughout all simulation examples. For the proposed control system, the γ value was kept the same as or larger than those of the other methods. Note that a control system with a larger γ value implies more robust stability.

Example 1 *(Vinante and Luyben (VL) Column).* A 24-tray tower separating a mixture of methanol and water, examined by Luyben [3],

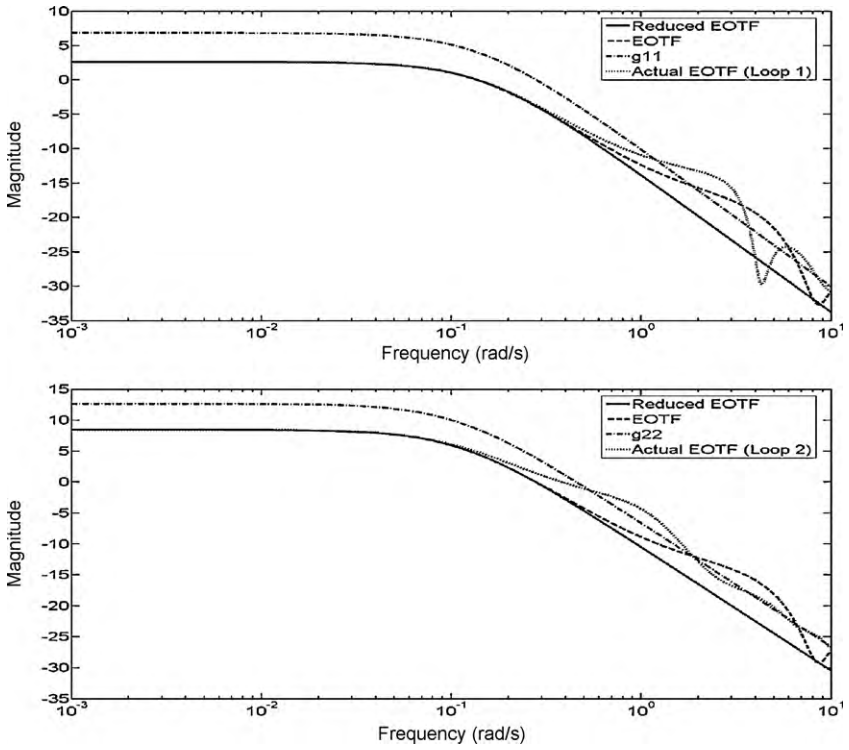

Fig. 3. Bode magnitude plots of the reduced EOTFs, EOTFs, g_{ii}, and actual EOTFs for the VL column.

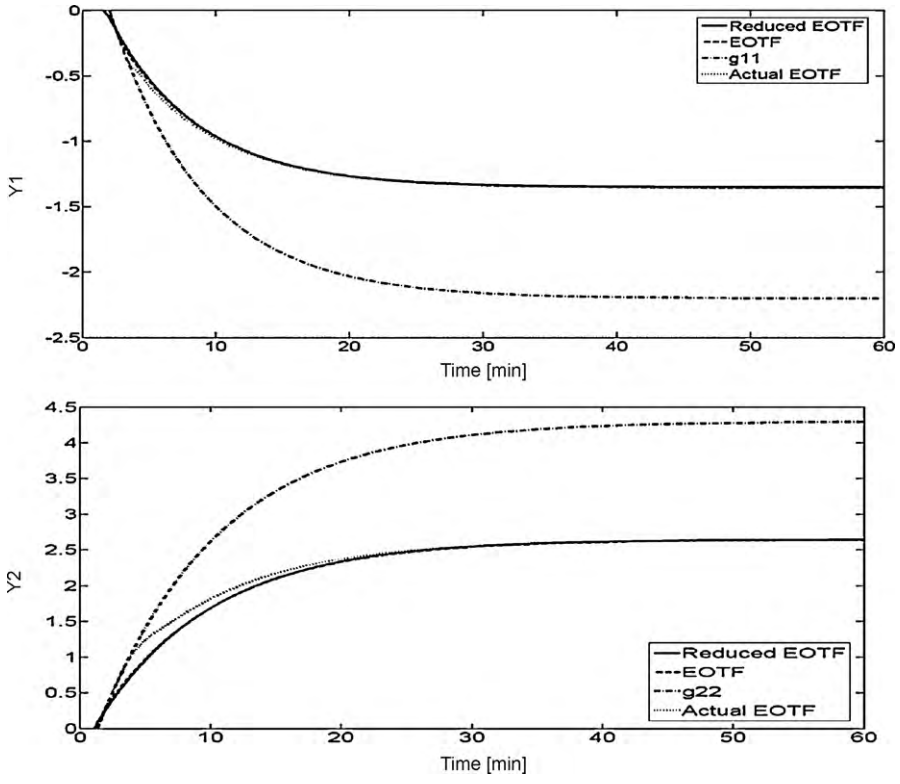

Fig. 4. The time responses of the reduced EOTFs, EOTFs, g_{ii}, and actual EOTFs for the VL column.

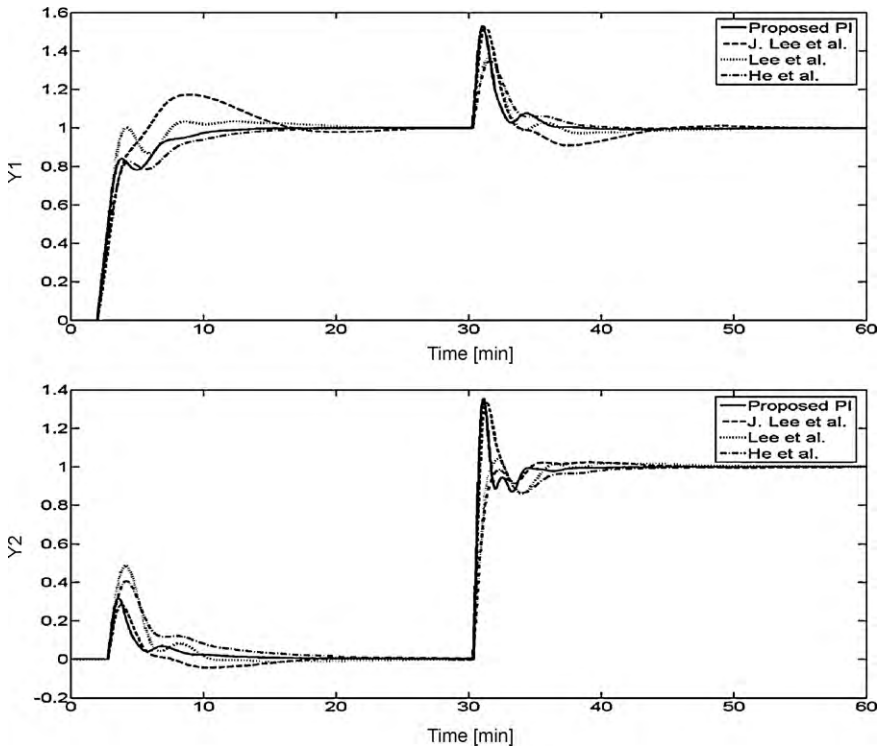

Fig. 5. Closed-loop responses to the sequential step changes in the set-point for the VL column.

has the following transfer function matrix

$$\mathbf{G}(s) = \begin{bmatrix} \dfrac{-2.2e^{-s}}{7s+1} & \dfrac{1.3e^{-0.3s}}{7s+1} \\ \dfrac{-2.8e^{-1.8s}}{9.5s+1} & \dfrac{4.3e^{-0.35s}}{9.2s+1} \end{bmatrix} \tag{33}$$

For this TITO system, it follows from (9) and (10) that the EOTFs for the first and second loops are obtained as

$$g_{11}^{\text{eff}}(s) = \frac{-2.2e^{-s}}{7s+1} + \frac{0.85(9.2s+1)e^{-1.75s}}{(7s+1)(9.5s+1)}; \quad g_{22}^{\text{eff}}(s) = \frac{4.3e^{-0.35s}}{9.2s+1} - \frac{1.65e^{-1.1s}}{9.5s+1}$$

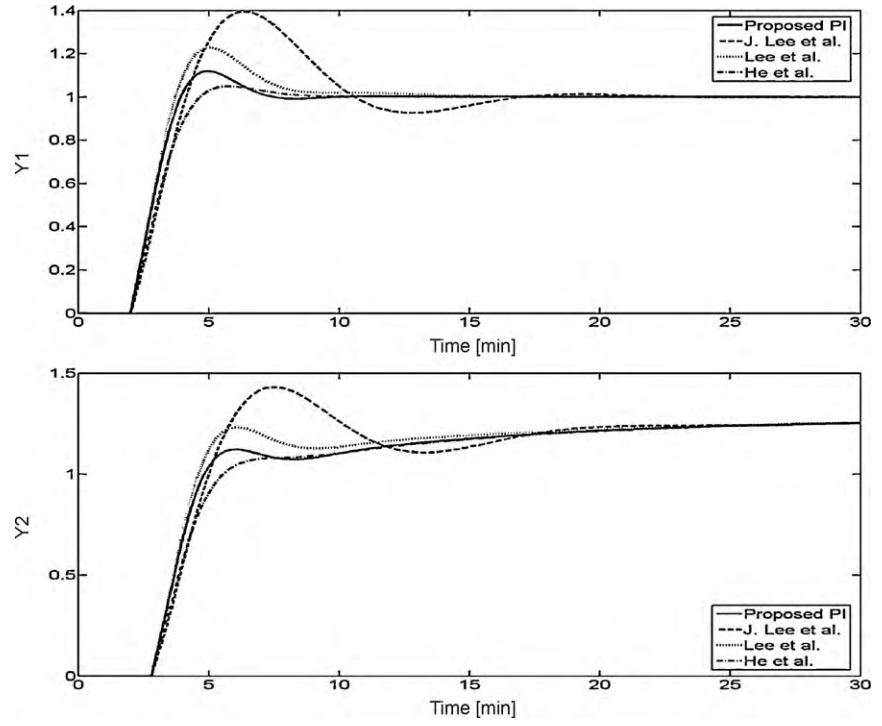

Fig. 6. Output responses of the VL column where loop 1 is closed and loop 2 is open.

Table 2
Controller parameters and resulting performance indices for the VL column.

Tuning method	Loop	K_{ci}	τ_{Ii}	τ_{Di}	λ_i	γ	IAE_t		
							Nominal	VL (+40%)	VL (−40%)
Proposed PID	1	−1.83	6.71	0.090	1.98	0.53	5.54	5.59	8.37
	2	5.54	8.84	0.002	0.55				
Proposed PI	1	−1.89	6.72	–	1.89	0.53	5.58	5.23	8.31
	2	5.20	8.84	–	0.59				
J. Lee et al.	1	−1.31	2.26	–	–	0.53	7.10	6.00	9.24
	2	3.97	2.42	–	–				
Lee et al.	1	−1.90	4.48	–	0.74	0.53	6.10	6.36	8.94
	2	2.45	5.70	–	0.53				
He et al.	1	−1.59	6.71	–	1.00	0.69	7.50	5.60	12.35
	2	2.28	8.84	–	0.35				

IAE_t: total sum of each loop's IAE. VL (+40%) and VL (−40%) denote the plant-model mismatch cases under +40 and −40% gain uncertainty, respectively.

The reduced EOTFs for the corresponding EOTFs are constituted using (21a)–(21c) as follows

$$g_{11}^{r\_\text{eff}} = \frac{-1.354e^{-0.682s}}{6.661s+1}; \quad g_{22}^{r\_\text{eff}} = \frac{2.646e^{-0.052s}}{8.841s+1}$$

To evaluate how closely the proposed reduced EOTF approximates the actual EOTF, the Bode diagrams and the time responses are drawn for several cases. Figs. 3 and 4 compare the Bode diagrams and the time responses of the reduced EOTF, EOTF, original OTF, and actual EOTF. From Fig. 3, both the reduced EOTF and EOTF show a fairly good coincidence with the actual EOTFs over the control relevant low and middle frequency ranges, becoming more conservative as the frequency increases. Note that the response of the actual EOTF is the actual response based on (3), and thus depends on the controller of other loops. Fig. 4 compares the time responses of the reduced EOTF, EOTF, original OTF, and actual EOTF. As seen from Fig. 4, the time response of the reduced EOTF is closely approximated to the actual EOTF. These close approximations to the actual EOTF in the frequency and time responses illustrate the validity of the EOTF and the reduced EOTF, and also essentially lead to satisfactory control performance of the multi-loop controller designed based on the EOTF. Furthermore, the significant difference between the original OTF, g_{ii}, and the other EOTFs confirm that the tuning of the individual multi-loop controller should be done based on the EOTF rather than the original OTF.

Fig. 5 shows the closed-loop responses by several tuning methods. In the simulation study, the unit step set-point changes were sequentially introduced into the individual loops. For both the proposed method and Lee et al.'s [44] method, λ_i was adjusted to have a degree of robust stability as $\gamma = 0.53$, which is the same as that obtained by Lee et al.'s [2] method and smaller than that of He et al. [16]. Note that since the method of He et al. [16] utilized the SIMC-PID tuning rule [45] by setting λ_i equal to θ_{ii}, their respective tuning values were employed in the simulation without adjusting the γ value. Fig. 6 compares the output responses afforded by the proposed method with those given by others where loop 1 is closed and loop 2 is open. The resulting controller parameters, together with the performance indices calculated using the above-mentioned methods, are summarized in Table 2. It is apparent from Figs. 5 and 6 that the proposed PI/PID controller provides a good performance with fast and well-balanced responses in comparison with those of the existing methods. The effectiveness of the proposed PI/PID controller is also confirmed by its smallest IAE value in Table 2.

The robustness of the controller is evaluated by inserting a perturbation uncertainty of ±40% in the process gain into the actual process, whereas the controller settings are those provided for the nominal process. The resulting performance index for the plant-model mismatch is tabulated in Table 2. As seen from the table, it is obvious that the proposed controller affords a good robust performance consistently.

Example 2 *(Wood and Berry (WB) Column).* Wood and Berry [46] introduced the following model of a pilot-scale distillation column consisting of an eight-tray plus reboiler separating methanol and water

$$\mathbf{G}(s) = \begin{bmatrix} \dfrac{12.8e^{-s}}{16.7s+1} & \dfrac{-18.9e^{-3s}}{21s+1} \\ \dfrac{6.6e^{-7s}}{10.9s+1} & \dfrac{-19.4e^{-3s}}{14.4s+1} \end{bmatrix} \tag{34}$$

Table 3
Controller parameters and resulting performance indices for the WB column.

Tuning method	Loop	K_{ci}	τ_{Ii}	τ_{Di}	λ_i	γ	IAE_t		
							Nominal	WB (+40%)	WB (−40%)
Proposed PID	1	0.66	10.55	0.02	2.20	0.47	19.13	19.17	27.42
	2	−0.11	7.54	1.04	2.87				
Proposed PI	1	0.50	10.54	–	3.00	0.47	22.45	23.49	32.72
	2	−0.09	7.32	–	4.41				
Ho et al.	1	0.57	20.70	–	–	0.47	29.70	26.62	49.56
	2	−0.11	12.88	–	–				
Lee et al.	1	0.24	8.36	–	4.55	0.47	25.70	29.97	37.66
	2	−0.10	7.46	–	4.55				
Loh et al.	1	0.87	3.25	–	–	0.33	24.60	23.82	36.20
	2	−0.09	10.40	–	–				

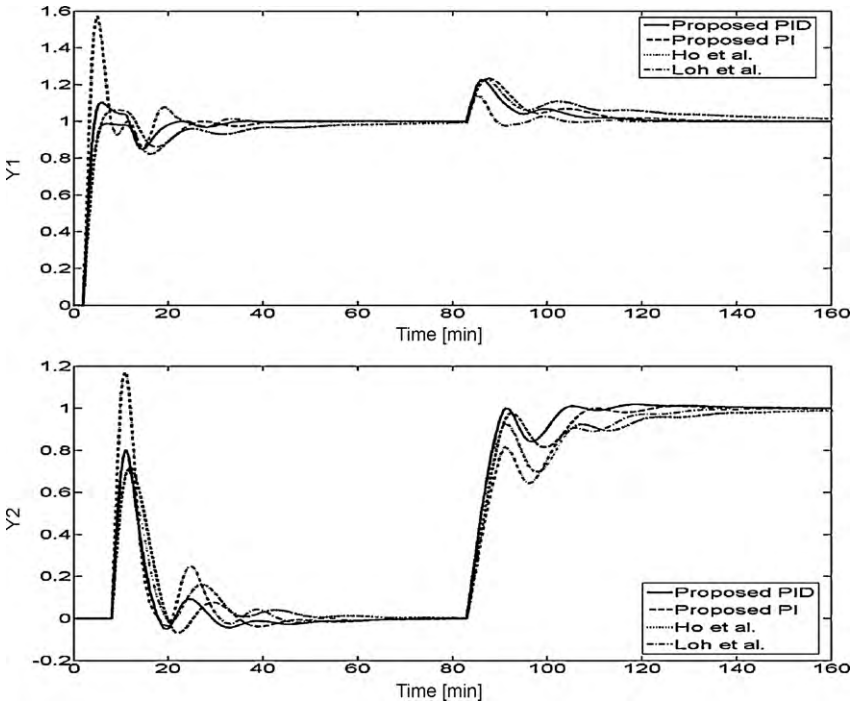

Fig. 7. Closed-loop responses to the sequential step changes in the set-point for the WB column.

The EOTFs for the first and second loops are found as

$$g_{11}^{\text{eff}}(s) = \frac{12.8e^{-s}}{16.7s+1} - \frac{6.36(14.4s+1)e^{-7s}}{(21s+1)(10.9s+1)}; \quad g_{22}^{\text{eff}}(s) = \frac{-19.4e^{-3s}}{14.4s+1} + \frac{9.75(16.7s+1)e^{-9s}}{(21s+1)(10.9s+1)}$$

The EOTFs are approximated to the reduced EOTFs by using the proposed model reduction method as follows

$$g_{11}^{r\_\text{eff}} = \frac{6.370e^{-0.308s}}{10.529s+1}; \quad g_{22}^{r\_\text{eff}} = \frac{-9.655e^{-4.265s}}{6.271s+1}$$

The multi-loop PI controller design methods suggested by Ho et al. [47], Lee et al. [44], and Loh et al. [8] were employed for the comparison as they have demonstrated effectiveness over other existing methods. The controller parameters used are listed in Table 3. For a fair comparison, the λ_i values for both the proposed method and that of Lee et al. [44] were adjusted for $\gamma = 0.47$, the same as the method of Ho et al. [47] and larger than that of Loh et al.'s [8] method.

Fig. 7 compares the closed-loop time responses by the proposed method and the above-mentioned design methods, where the unit step changes in the set-point were sequentially made at $t = 0$ and $t = 80$ to the 1st and 2nd loops, respectively. The performance indices are also tabulated in Table 3. The good performance of the proposed method is readily apparent.

To demonstrate the robust performance of the proposed method, the simulation study was also done by inserting a perturbation uncertainty of ±40% in process gain. As shown in Table 3, the controller settings of the proposed method provide a good robust performance for the set-point change.

Example 3 *(Ogunnaike and Ray (OR) Column).* The multi-product plant distillation column for the separation of a binary ethanol–water mixture was modeled experimentally by Ogunnaike

Table 4
Controller parameters and resulting performance indices for the OR column.

Tuning method	Loop	K_{ci}	τ_{Ii}	τ_{Di}	τ_{Fi}	λ_i	γ	IAE_t
Proposed PID	1	2.25	7.12	2.58	4.37	8.00	0.06	268.3
	2	−0.49	6.44	3.37	5.65	5.00		
	3	4.83	3.11	10.16	5.74	0.05		
BLT	1	1.51	16.40	–	–	–	0.035	361.7
	2	−0.30	18.00	–	–	–		
	3	2.63	6.61	–	–	–		
DLT	1	0.96	8.00	1.09	1.03	10.00	0.037	505.6
	2	−0.20	6.50	1.15	1.15	10.00		
	3	2.37	11.00	3.22	11.61	10.00		
Halevi et al.	1	1.25	10.50	–	–	–	0.035	982.8
	2	−0.30	10.50	–	–	–		
	3	0.92	10.50	–	–	–		
Jung et al.	1	1.59	6.58	6.66	10.2	10.00	0.030	862.9
	2	−0.40	7.40	5.50	11.3	10.00		
	3	1.24	8.08	3.84	5.57	10.00		

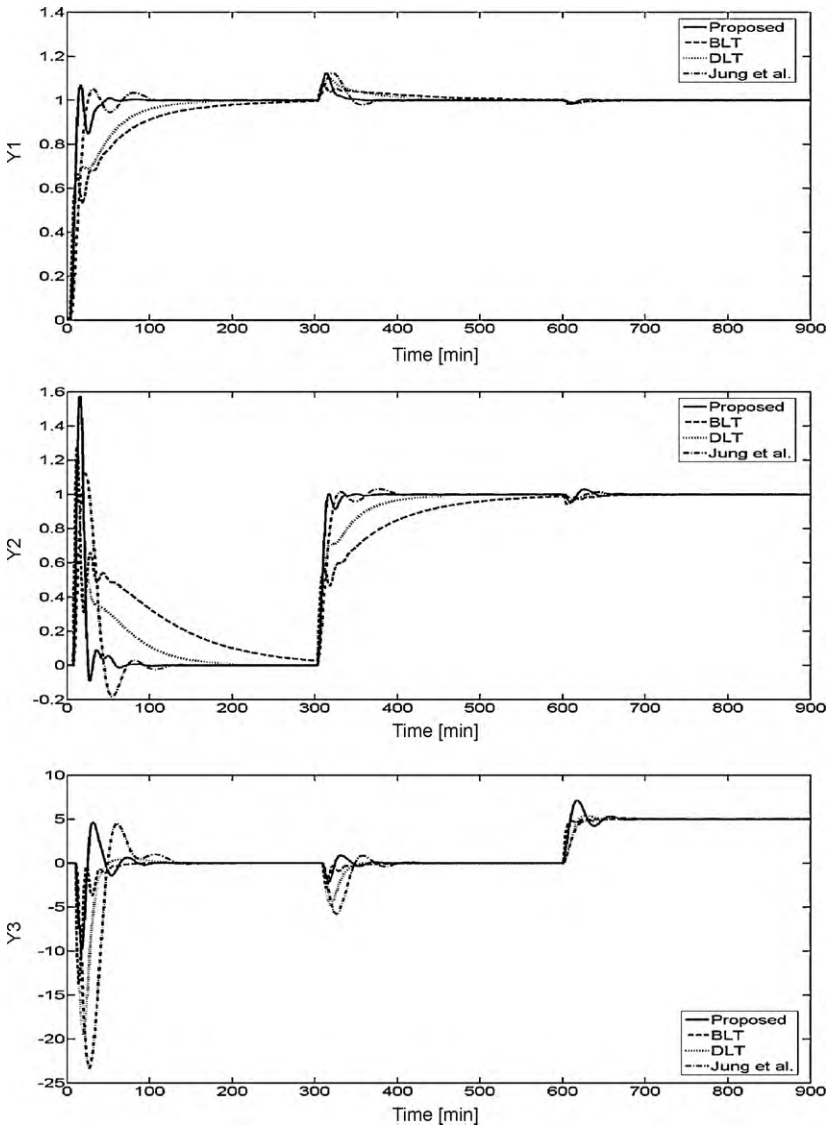

Fig. 8. Closed-loop responses to the sequential step changes in the set-point for the OR column.

et al. [48], the open-loop transfer function matrix is given by

$$\mathbf{G}(s) = \begin{bmatrix} \dfrac{0.66e^{-2.6s}}{6.7s+1} & \dfrac{-0.61e^{-3.5s}}{8.64s+1} & \dfrac{-0.0049e^{-s}}{9.06s+1} \\ \dfrac{1.11e^{-6.5s}}{3.25s+1} & \dfrac{-2.36e^{-3s}}{5s+1} & \dfrac{-0.01e^{-1.2s}}{7.09s+1} \\ \dfrac{-34.68e^{-9.2s}}{8.15s+1} & \dfrac{46.2e^{-9.4s}}{10.9s+1} & \dfrac{0.87(11.61s+1)e^{-s}}{(3.89s+1)(18.8s+1)} \end{bmatrix} \tag{35}$$

In this example, since a simple FOPDT model did not take major process interactions into account, the SOPDT model with a lead term was chosen as the reduced EOTF model. The reduced EOTFs are constituted as follows

$$g_{11}^{r\_\text{eff}} = \frac{0.34(13.83s+1)e^{-2.1s}}{(12.62s+1)(3.73s+1)}; \quad g_{22}^{r\_\text{eff}} = \frac{-1.25(17.28s+1)e^{-2.62s}}{(14.89s+1)(2.84s+1)}; \quad g_{33}^{r\_\text{eff}} = \frac{0.57(17.46s+1)e^{-1.08s}}{(10.51s+1)(3.80s+1)}$$

For a SOPDT model with negative zero, the PID controller in series with the first-order lag filter structure was recommended to enhance the closed-loop performance. In the simulation study, the λ_i values of the proposed method were chosen to obtain the $\gamma = 0.06$, which gives a higher robustness level than those of the BLT [3], Halevi et al.'s [10], decentralized lambda tuning (DLT) [14], and Jung et al.'s [14] methods. The controller parameters used are given in Table 4.

Fig. 8 shows the closed-loop time response of the proposed method in comparison with those by BLT [3], DLT [14], and Jung et al.'s [14] methods, where the magnitudes of the sequential step changes in the set-point of loops 1, 2, and 3 are 1, 1, and 5, respectively. A multi-loop PID controller in series with a first-order lag filter structure was used for the proposed, DLT [14], and Jung et al.'s [14] methods, whereas the standard PI controller structure was utilized for the BLT [3] method. The order of the IMC filter was chosen as 1 for all loops. It is clear from Fig. 8 that the PID controller obtained by the proposed method yielded fast and well-balanced responses. The performance indices of all the comparative methods are also tabulated in Table 4, of which the smallest total IAE value was found for the closed-loop response provided by the proposed method in terms of higher robustness level than other methods.

6. Conclusion

A novel method for the independent design of a multi-loop PID controller is proposed, based on the concept of EOTF. The EOTF concept was successfully applied to decompose the complex multi-loop control systems into a number of independent SISO loops in which dynamic interaction is taken into account. Therefore, the multi-loop PID controller was accomplished by designing the SISO PI/PID controllers for each loop based on the corresponding EOTF model. It was also shown that the well-known DRGA was interpreted as a ratio of the OTF to the EOTF. A model reduction technique was proposed to further simplify the EOTF to the reduced-order form. The IMC-PID approach [41] was applied to the reduced EOTF to design the individual PI/PID controller in each loop.

Results from the frequency and time response analysis confirm that the EOTF and the reduced EOTF closely approximate the dynamic interaction among loops and the actual EOTF. A simulation study was also carried out to evaluate the proposed approach. In order to insure a fair comparison, the maximum upper bound on the singular values of the output multiplicative uncertainty for the robust stability was utilized as a measure of the robustness level. The simulation results indicate that the proposed method consistently affords a good performance with a fast and well-balanced closed-loop time response. Robustness study was also conducted by inserting a perturbation uncertainty of ±40% in the process gain. The results showed that the proposed control systems held robust stability well in the plant-model mismatch case.

Acknowledgment

This research was supported by a grant from the Gas Plant R&D Center funded by the Ministry of Land, Transportation and Maritime Affairs (MLTM) of the Korean government.

Appendix A.

From the properties of matrix

$$\mathbf{G}(\mathrm{adj}\mathbf{G}) = |\mathbf{G}|\mathbf{I} \tag{A.1}$$

where $\mathbf{I}$ denotes the identity matrix, $|\mathbf{G}|$ the determinant of $\mathbf{G}$, and adj$\mathbf{G}$ the adjoint of $\mathbf{G}$, and the transpose of the matrix of cofactors corresponding to the entries of $\mathbf{G}$

$$\mathrm{adj}\mathbf{G} = \begin{pmatrix} C_{11} & C_{21} & \dots & C_{n1} \\ C_{12} & C_{22} & \dots & C_{n2} \\ \vdots & \vdots & & \vdots \\ C_{1n} & C_{2n} & \dots & C_{nn} \end{pmatrix} \tag{A.2}$$

From (A.1), it is implied that

$$g_{i1}C_{i1} + \cdots + g_{i,i-1}C_{i,i-1} + g_{ii}C_{ii} + g_{i,i+1}C_{i,i+1} + \cdots + g_{in}C_{in} = |\mathbf{G}| \tag{A.3}$$

$$\begin{bmatrix} g_{11} & \cdots & g_{1,i-1} & g_{1,i} & g_{1,i+1} & \cdots & g_{1,n} \\ \vdots & & \vdots & \vdots & \vdots & & \vdots \\ g_{i-1,1} & \cdots & g_{i-1,i-1} & g_{i-1,i} & g_{i-1,i+1} & \cdots & g_{i-1,n} \\ g_{i+1,1} & \cdots & g_{i+1,i-1} & g_{i+1,i} & g_{i+1,i+1} & \cdots & g_{i+1,n} \\ \vdots & & \vdots & \vdots & \vdots & & \vdots \\ g_{n1} & \cdots & g_{n,i-1} & g_{n,i} & g_{n,i+1} & \cdots & g_{nn} \end{bmatrix} \begin{bmatrix} C_{i1} \\ \vdots \\ C_{i,i-1} \\ C_{i,i} \\ C_{i,i+1} \\ \vdots \\ C_{i,n} \end{bmatrix} = \begin{bmatrix} 0 \\ \vdots \\ 0 \\ 0 \\ \vdots \\ 0 \end{bmatrix} \tag{A.4}$$

where g_{ij} and C_{ij} denote the ijth element of $\mathbf{G}$ and its cofactor, respectively.

From (A.3), the ith diagonal element of $\mathbf{G}$ is written as

$$g_{ii} = \frac{1}{C_{ii}}[|\mathbf{G}| - (g_{i1}C_{i1} + g_{i2}C_{i2} + \cdots + g_{i,i-1}C_{i,i-1} + g_{i,i+1}C_{i,i+1} + \cdots + g_{in}C_{in})] = \frac{|\mathbf{G}|}{C_{ii}} - \frac{\bar{\mathbf{g}}^{ir}\bar{\mathbf{C}}^{ic}}{C_{ii}} \tag{A.5}$$

where $\bar{\mathbf{C}}^{ic} = [C_{i1}\ C_{i2} \dots C_{i,i-1}\ C_{i,i+1} \dots C_{in}]^T$.

Note that $\bar{\mathbf{C}}^{ic}$ corresponds to the ith column vector of adj$\mathbf{G}$ dropping the element C_{ii}.

(A.4) is rearranged as

$$\bar{\mathbf{G}}^{i}\bar{\mathbf{C}}^{ic} + \bar{\mathbf{g}}^{ic}C_{ii} = 0 \tag{A.6}$$

Thus,

$$\bar{\mathbf{g}}^{ic} = -\frac{\bar{\mathbf{G}}^{i}\bar{\mathbf{C}}^{ic}}{C_{ii}} \tag{A.7}$$

Substituting (A.5) and (A.7) into (4), the EOTF is expressed as

$$g_{ii}^{\mathrm{eff}} = \left(\frac{|\mathbf{G}|}{C_{ii}} - \frac{\bar{\mathbf{g}}^{ir}\bar{\mathbf{C}}^{ic}}{C_{ii}}\right) - \bar{\mathbf{g}}^{ir}(\bar{\mathbf{G}}^{i})^{-1}\left(-\frac{\bar{\mathbf{G}}^{i}\bar{\mathbf{C}}^{ic}}{C_{ii}}\right) = \frac{|\mathbf{G}|}{C_{ii}} \tag{A.8}$$

Furthermore, each diagonal element of the DRGA matrix is calculated as

$$\Lambda_{ii} = g_{ii}\frac{C_{ii}}{|\mathbf{G}|} \tag{A.9}$$

Therefore, rearranging (A.9) for $|\mathbf{G}|$ and substituting it into (A.8) leads to

$$g_{ii}^{\mathrm{eff}} = \frac{g_{ii}}{\Lambda_{ii}} \tag{A.10}$$

References

[1] P.J. Campo, M. Morari, Achievable closed-loop properties of systems under decentralized control: conditions involving the steady-state gain, IEEE Trans. Automat. Control 39 (1994) 932–943.
[2] J. Lee, W. Cho, T.F. Edgar, Multi-loop PI controller tuning for interacting multivariable processes, Comput. Chem. Eng. 22 (1998) 1711–1723.
[3] W.L. Luyben, Simple method for tuning SISO controllers in multivariable systems, Ind. Eng. Chem. Process Des. Dev. 25 (1986) 654–660.
[4] J.G. Ziegler, N.B. Nichols, Optimum settings for automatic controllers, Trans. ASME 64 (1942) 759–768.
[5] D.Q. Mayne, The design of linear multivariable systems, Automatica 9 (1973) 201–207.
[6] M. Hovd, S. Skogestad, Sequential design of decentralized controllers, Automatica 30 (1994) 1601–1607.
[7] K.J. Åström, T. Hägglund, Automatic Tuning of PID Controllers, Instrument Society of America, Research Triangle Park, NC, 1988.
[8] A.P. Loh, C.C. Hang, C.K. Quek, V.U. Vasnani, Auto-tuning of multi-loop proportional-integral controllers using relay feedback, Ind. Eng. Chem. Res. 32 (1993) 1102–1107.
[9] S.H. Shen, C.C. Yu, Use of relay-feedback test for automatic tuning of multivariable systems, AIChE J. 40 (1994) 627–646.
[10] Y. Halevi, Z.J. Palmor, T. Efrati, Automatic tuning of decentralized PID controllers for MIMO processes, J. Process Control 7 (1997) 119–128.
[11] P. Grosdidier, M. Morari, Interaction measures for systems under decentralized control, Automatica 22 (1986) 309–320.
[12] S. Skogestad, M. Morari, Robust performance of decentralized control system by independent design, Automatica 25 (1989) 119–125.
[13] M. Hovd, S. Skogestad, Improved independent design of robust decentralized controllers, J. Process Control 3 (1) (1993) 43–51.
[14] J. Jung, J.Y. Choi, J. Lee, One parameter method for a multi-loop control system design, Ind. Eng. Chem. Res. 38 (1999) 1580–1588.
[15] Z.X. Zhu, Structural analysis and stability conditions of decentralized control systems, Ind. Eng. Chem. Res. 35 (1996) 736–745.
[16] M.-J. He, W.J. Cai, B.F. Wu, M. He, Simple decentralized PID controller design method based on dynamic relative interaction analysis, Ind. Eng. Chem. Res. 44 (2005) 8334–8344.
[17] H.P. Huang, J.C. Jeng, C.H. Chiang, W. Pan, A direct method for multi-loop PI/PID controller design, J. Process Control 13 (2003) 769–786.
[18] Q. Xiong, W.-J. Cai, Effective transfer function method for decentralized control system design of multi-input multi-output processes, J. Process Control 16 (2006) 773–784.

[19] H. Cui, E.W. Jacobsen, Performance limitations in decentralized control, J. Process Control 12 (2002) 485–494.
[20] E.H. Bristol, On a new measure of interactions for multivariable process control, IEEE Trans. Automat. Control 11 (1966) 133–134.
[21] M.F. Witcher, T.J. McAvoy, Interacting control systems: steady-state and dynamic measurement of interaction, ISA Trans. 16 (1977) 35–41.
[22] E.H. Bristol, Recent results on interactions in multivariable process control, in: Proceedings of the 71st Annual AIChE Meeting, Houston, TX, USA, 1979.
[23] L.S. Tung, T.F. Edgar, Analysis of control-output interaction in dynamic systems, AIChE J. 27 (1981) 690–693.
[24] S. Skogestad, I. Poslethwaite, Multivariable Feedback Control, John Wiley and Sons, New York, 1996.
[25] Q. Xiong, W.-J. Cai, M.-J. He, A practical loop pairing criterion for multivariable process, J. Process Control 15 (2005) 741–747.
[26] M.-J. He, W.-J. Cai, W. Ni, L.-H. Xie, RNGA based control system configuration for multivariable processes, J. Process Control 19 (2009) 1036–1042.
[27] F. Shinskey, Process Control System, McGraw-Hill, New York, 1979.
[28] W.L. Luyben, Process Modeling, Simulation and Control for Chemical Engineers, McGraw-Hill, New York, 1990.
[29] T. Liu, W. Zhang, D. Gu, Analytical multi-loop PI/PID controller design for two-by-two processes with time delays, Ind. Eng. Chem. Res. 44 (6) (2005) 1832–1841.
[30] V. Strejc, Least squares parameter estimation, Automatica 16 (5) (1980) 535–550.
[31] R. Pintelon, P. Guillaume, Y. Rolain, J. Schoukens, H.V. Hamme, Parametric identification of transfer functions in the frequency domain – a survey, IEEE Trans. Automat. Control 39 (11) (1994) 2245–2260.
[32] B. Ninness, Integral constraints on the accuracy of least squares estimation, Automatica 32 (2) (1996) 391–397.
[33] P.J. Gawthrop, M.T. Nihtila, Identification of time-delays using a polynomial identification method, Syst. Control Lett. 5 (1985) 267–271.
[34] R. Malti, S.B. Ekongolo, J. Ragot, S.I.S.O. Dynamic, MIMO system approximation based on optimal Laguerre methods, IEEE Trans. Automat. Control 43 (9) (1998) 1318–1323.
[35] C.C. Zervos, G.A. Dumont, Deterministic adaptive control based on Laguerre series representation, Int. J. Control 48 (1988) 2333–2359.
[36] H.I. Park, S.W. Sung, I.-B. Lee, J. Lee, On-line process identification using the Laguerre series for automatic tuning of the proportional-integral-derivative controller, Ind. Eng. Chem. Res. 36 (1997) 101–111.
[37] R. Pintelon, L.V. Biesen, Identification of transfer functions with time delay and its application to cable fault location, IEEE Trans. Instrum. Meas. 39 (6) (1990) 479–484.
[38] F.-S. Wang, W.-S. Juang, C.-T. Chan, Optimal tuning of PID controllers for single and cascade control loops, Chem. Eng. Commun. 132 (1995) 15–34.
[39] Q.-G. Wang, Y. Zhang, X. Guo, Robust closed-loop identification with application to auto-tuning, J. Process Control 11 (5) (2001) 519–530.
[40] M. Shamsuzzoha, M. Lee, Design of advanced PID controller for enhanced disturbance rejection of second-order processes with time delay, AIChE J. 54 (6) (2008) 1526–1536.
[41] Y. Lee, S. Park, M. Lee, C. Brosilow, PID controller tuning for desired closed-loop responses for SI/SO systems, AIChE J. 44 (1) (1998) 106–115.
[42] S.L. William, Control System Fundamentals, CRC Press, 1999.
[43] J. Lee, D.H. Kim, T.F. Edgar, Static decouplers for control of multivariable processes, AIChE J. 51 (10) (2005) 2712–2720.
[44] M. Lee, K. Lee, C. Kim, J. Lee, Analytical design of multi-loop PID controllers for desired closed-loop responses, AIChE J. 50 (2004) 1631–1635.
[45] S. Skogestad, Simple analytic rules for model reduction and PID controller tuning, J. Process Control 13 (2003) 291–309.
[46] R.K. Wood, M.W. Berry, Terminal composition control of binary distillation column, Chem. Eng. Sci. 28 (1973) 1707–1717.
[47] W.H. Ho, T.H. Lee, O.P. Gan, Tuning of multi-loop PID controllers based on gain and phase margin specifications, Ind. Eng. Chem. Res. 36 (1997) 2231–2238.
[48] B.A. Ogunnaike, J.P. Lemaire, M. Morari, W.H. Ray, Advanced multivariable control of a pilot plant distillation column, AIChE J. 29 (1983) 632–640.